From Anderson to anomalous localization in cold atomic gases with effective spin–orbit coupling

2012 New J. Phys. 14 073056

(http://iopscience.iop.org/1367-2630/14/7/073056)

New Journal of Physics
The open-access journal for physics

From Anderson to anomalous localization in cold atomic gases with effective spin–orbit coupling

M J Edmonds[1,5], J Otterbach[2,5], R G Unanyan[3], M Fleischhauer[3], M Titov[1,4] and P Öhberg[1]

[1] SUPA, Department of Physics, Heriot-Watt University, Edinburgh EH14 4AS, UK
[2] Physics Department, Harvard University, Cambridge, 02139 MA, USA
[3] Department of Physics and Research Center OPTIMAS, Technische Universität Kaiserslautern, 67663 Kaiserslautern, Germany
[4] Institut für Nanotechnologie, Karlsruhe Institute of Technology, 76021 Karlsruhe, Germany
E-mail: mje9@hw.ac.uk and jotterbach@physics.harvard.edu

New Journal of Physics **14** (2012) 073056 (11pp)
Received 3 April 2012
Published 31 July 2012
Online at http://www.njp.org/
doi:10.1088/1367-2630/14/7/073056

Abstract. We study the dynamics of a spin–orbit (SO)-coupled Schrödinger particle with two internal degrees of freedom moving in a one-dimensional random potential. Numerical calculation of the density of states reveals the emergence of a Dyson-like singularity at zero energy when the system approaches the quasi-relativistic limit of the random-mass Dirac model for large SO coupling. Simulations of the expansion of an initially localized wave-packet show a crossover from an exponential (Anderson) localization to an anomalous power-law behavior reminiscent of the zero-energy (mid-gap) state of the random-mass Dirac model. We discuss conditions under which the crossover is observable in an experiment and derive the zero-energy state, thus proving its existence under proper conditions. Finally we describe a possible experimental realization using an ensemble of cold ^{87}Rb-atoms interacting with external control lasers and speckle fields.

[5] Authors to whom any correspondence should be addressed.

Contents

1. Introduction

Tightly confined ultracold atomic gases [1] provide an ideal arena for studying a broad spectrum of one-dimensional (1D) quantum phenomena. Examples range from Hubbard-type models [2, 3], pairing phenomena in Fermi gases [4, 5] to spin–orbit (SO) coupling for neutral atoms [6–9] and quasi-relativistic physics [10, 11], generated by the additional use of external laser fields. The same experimental techniques can also be used to address the effects of disorder in condensed matter systems in an atomic-physics setting. A prominent example is the demonstration of Anderson localization [12] of a Bose–Einstein condensate (BEC) in a 1D wave-guide [13, 14]. One-dimensional Anderson localization is caused by destructive interference in a weak, disordered potential (referred to as diagonal disorder) and leads to exponential localization of the particles [15–18]. This behavior may change in half-filled disordered metals [19], random spin-Peierls and spin-ladder systems [20], or as recently predicted in photonic systems with electromagnetically induced transparency [21]. Delocalized zero-energy (mid-gap) states can emerge in these systems showing a power-law behavior for the correlations due to a Dyson singularity in the density of states (DOS) [22]. Such anomalous localization originates from the chiral symmetry of the corresponding 1D Hamiltonian and can be realized in the system with off-diagonal disorder known as a random-mass Dirac model or the fluctuating gap model (FGM) [23–26]. The singularity in the DOS was discovered in 1953 by Freeman Dyson [27] who calculated the density of phonon modes in a chain of 1D harmonic oscillators with random masses and random couplings. It emerges at the band-center and strongly affects the localization properties, leading to a diverging localization length at $E = 0$. However, as was shown by Fleishman and Licciardello [31] the $E = 0$ state is not extended due to strong fluctuations. In fact, it can be shown that there exists a Dyson singularity for any distribution of off-diagonal disorder [29, 30]. Interestingly, the FGM can also be mapped onto a chain of identical atoms with a random XY model [28].

In cold atom systems disorder is typically induced by a random potential and is thus of diagonal type. Here we show that the combination of a random potential and SO coupling induced by the motion in space dependent laser fields can give rise to effective off-diagonal disorder. Light-induced SO coupling has been shown to lead to an effective Dirac dynamics in [11]. By investigating the density of states of the corresponding disorder model we derive conditions under which power-law localization can be observed and argue that they are indeed connected to the emergence of a Dyson singularity in the DOS. We show by simulating the time evolution of an initially localized wave packet that increasing the SO coupling drives a crossover from exponential (Anderson) localization to an anomalous power-law localization.

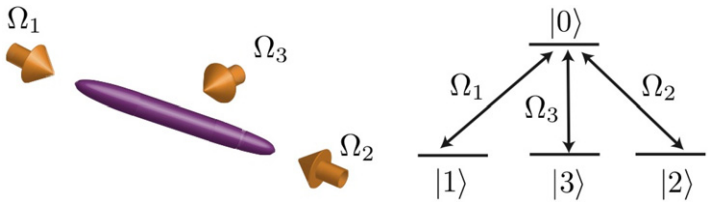

Figure 1. Left: experimental sketch of the system. The condensate is placed in a tight cigar-shaped trap and driven by three lasers with Rabi frequencies Ω_1, Ω_2 and Ω_3. Right: internal tripod-type linkage pattern of the atoms exhibiting two dark-states without any contribution of the excited state $|0\rangle$.

We note that a model similar to ours was considered in [32], but only for the case of diagonal disorder and neglecting the kinetic energy part. As will be shown the latter can be neglected only under special circumstances and drastically alters the behavior of the system, leading to much richer physics.

2. Dark-state dynamics for tripod coupling

We consider an ensemble of cold atoms exposed to three laser fields in a tripod-type linkage pattern [33], as depicted in figure 1. The atoms are characterized by a manifold of three ground states $|1\rangle$, $|2\rangle$, $|3\rangle$, coupled to a common excited state $|0\rangle$ via corresponding control lasers of wave-number κ. We assume two of the control lasers to be counter-propagating along the x-axis with Rabi frequencies $\Omega_1 = \Omega \sin\theta\, \mathrm{e}^{-\mathrm{i}\kappa x}/\sqrt{2}$ and $\Omega_2 = \Omega \sin\theta\, \mathrm{e}^{\mathrm{i}\kappa x}/\sqrt{2}$, whereas the third laser propagates along the y-axis with $\Omega_3 = \Omega \cos\theta\, \mathrm{e}^{-\mathrm{i}\kappa y}$, and $\Omega = \sqrt{\sum_{i=1}^{3} |\Omega_i|^2}$ denotes the total Rabi frequency. Following [33] we can write the interaction Hamiltonian ($\hbar = 1$) of the resulting tripod scheme as $\hat{H}_0 = -\sum_{i=1}^{3}(\Omega_i |0\rangle\langle i| + \mathrm{h.c.})$. This Hamiltonian has two dark-states, $|D_1\rangle = \frac{1}{\sqrt{2}}\mathrm{e}^{-\mathrm{i}\kappa y}(\mathrm{e}^{\mathrm{i}\kappa x}|1\rangle - \mathrm{e}^{-\mathrm{i}\kappa x}|2\rangle)$ and $|D_2\rangle = \frac{1}{\sqrt{2}}\mathrm{e}^{-\mathrm{i}\kappa y}\cos\theta(\mathrm{e}^{\mathrm{i}\kappa x}|1\rangle + \mathrm{e}^{-\mathrm{i}\kappa x}|2\rangle) - \sin\theta|3\rangle$, with zero energy and decoupled from the excited state $|0\rangle$. We express a general state of the system in the dark state manifold according to $|\chi(\mathbf{r})\rangle = \sum_{i=1}^{2} \psi_i(\mathbf{r})|D_i(\mathbf{r})\rangle$, where $\psi_1(\mathbf{r})$ and $\psi_2(\mathbf{r})$ are the wave functions corresponding to the two degenerate dark states. An effective equation for the center-of-mass amplitudes $\psi_i(\mathbf{r})$ is then given by [10]

$$\mathrm{i}\frac{\partial \boldsymbol{\Psi}}{\partial t} = \left(\frac{1}{2m}(\mathbf{p} - \mathbf{A})^2 + \mathbf{V} + \boldsymbol{\Phi}\right)\boldsymbol{\Psi}, \tag{1}$$

where $\mathbf{p}$ is the momentum operator, m the atomic mass, and $\boldsymbol{\Psi}(\mathbf{r}) = (\psi_1(\mathbf{r}), \psi_2(\mathbf{r}))^T$ a two-component vector. The gauge potential $\mathbf{A}$, known as the Mead–Berry connection [34, 35], arises from the coordinate-dependence of the dark-states and is given by $\mathbf{A}_{k,n} = \mathrm{i}\langle D_k(\mathbf{r})|\nabla|D_n(\mathbf{r})\rangle$. The external potential has matrix elements $\mathbf{V}_{k,n} = \langle D_k(\mathbf{r})|\hat{V}|D_n(\mathbf{r})\rangle$, where the potential in the bare basis was assumed to be diagonal, i.e. $\hat{V} = \sum_{i=1}^{3} V_i(\mathbf{r})|i\rangle\langle i|$. The scalar potential reads $\boldsymbol{\Phi}_{k,n} = \sum_{l=3}^{4} \mathbf{A}_{k,l}\mathbf{A}_{l,n}/2m$, where the summation index $l = 3, 4$ sums over the bright-states that span the orthogonal complement of the dark-subspace.

Up to this point the motion of the atoms has not been confined by any further potential. As we aim to study a 1D gas which is subject to an off-diagonal disorder, we apply an additional strong transverse trapping potential to freeze out the transverse degrees of freedom.

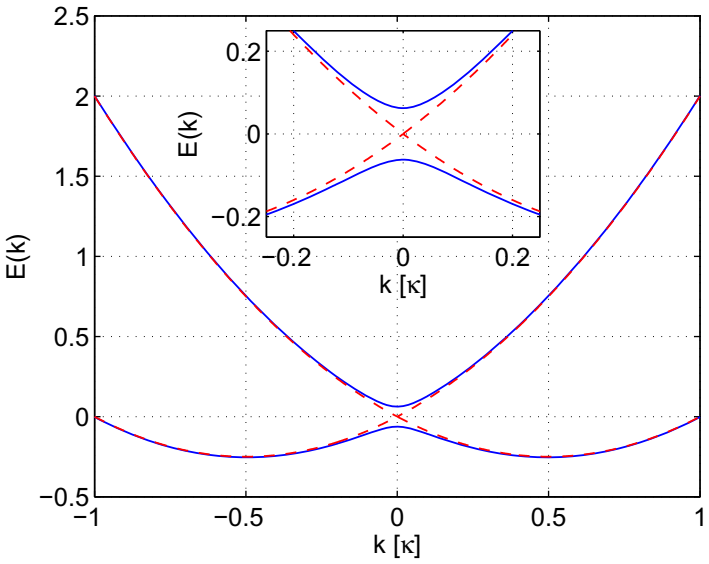

Figure 2. Dispersion relation in the Schrödinger limit, with the inset representing the Dirac limit. The red dotted lines correspond to the case of vanishing potential, i.e. $\delta = 0$, whereas the blue solid lines correspond to $\delta = m v_{\mathrm{D}}^2/8$. The mixing angle is given by $\theta = 0$.

Note that the recoil along the y-direction due to the $\mathrm{e}^{\mathrm{i}\kappa y}$-terms is then irrelevant, which however does not prevent the coupling of the field to the atoms. Equation (1) reduces to a 1D equation with 2×2-matrices $\mathbf{A} = -\kappa \cos\theta\, \hat{\sigma}_x$, $\mathbf{V} = \mathrm{Diag}[V_1, V_1 \cos^2\theta + V_3 \sin^2\theta]$, and $\mathbf{\Phi} = \kappa^2/2m\, \mathrm{Diag}[\sin^2\theta, \sin^2(2\theta)/4]$, where $\hat{\sigma}_i$, $i \in \{x, y, z\}$, are the Pauli matrices, and we have assumed $V_1 = V_2$. Reducing the center of mass dynamics to 1D is a valid approximation as long as the transversal trap frequency is much larger than any other energy scale in the system such as temperature, collisional interactions and kinetic energy. Expanding the square in equation (1) and choosing the external potentials as $V_1 = \Delta(x) - \kappa^2/2m$, and $V_3 = -\Delta(x)(1+\cos^2\theta)/(1-\cos^2\theta) - \kappa^2 \cos^2\theta/2m$, where $\Delta(x)$ is a detuning we arrive at

$$\mathrm{i}\frac{\partial \mathbf{\Psi}}{\partial t} = \left(\frac{\mathbf{p}_x^2}{2m} + v_{\mathrm{D}} \cos\theta\, \mathbf{p}_x \cdot \hat{\sigma}_x + \Delta(x)\hat{\sigma}_z\right)\mathbf{\Psi}, \tag{2}$$

with $v_{\mathrm{D}} = \kappa/m$. Note that the potential V_3 cannot be realized experimentally in the limit $\cos\theta = 1$. However, by proper choice of the parameters, one can approach this limit sufficiently closely. Equation (2) describes a massive particle with SO coupling moving in a scalar potential $\Delta(x)$. The corresponding dispersion relation for a constant potential $\Delta(x) = \delta$ can easily be calculated and is shown in figure 2 for the case of $\delta = 0$ (red dashed line) and small $\delta \neq 0$ (blue solid line). By changing the relative intensity of the control lasers one can externally control the value of $\cos\theta$ enabling an easy access to tune the effective SO coupling. In case of a smooth potential and large particle-momenta, i.e. $\langle \mathbf{p}_x^2 \rangle/2m \gg v_{\mathrm{D}} \langle \mathbf{p}_x \rangle \cos\theta$, the SO coupling becomes negligible and the problem reduces to two uncoupled massive Schrödinger particles moving in an external potential. In the opposite limit, i.e. for $\langle \mathbf{p}_x^2 \rangle/2m \ll v_{\mathrm{D}} \langle \mathbf{p}_x \rangle \cos\theta$, equation (2) reduces to an effective Dirac equation for a particle with an effective speed of light $c_* = v_{\mathrm{D}} \cos\theta$ and a smooth space-dependent mass $\Delta(x)/c_*^2$ [10, 11].

We assume in the following that the random potential is described by local, Gaussian white noise with

$$\overline{\Delta(x)\Delta(x')} = \Gamma v_{\mathrm{D}} \delta(x - x'), \quad \overline{\Delta(x)} = 0, \tag{3}$$

where the overbar denotes disorder average and all higher order correlation functions factorize. For vanishing SO coupling one expects exponential localization of the particles according to the Anderson scenario [13, 14, 22, 36, 37]. On the other hand, any small SO coupling dominates in the region of small kinetic energy. Neglecting the kinetic energy term proportional to $\langle \mathbf{p}_x^2 \rangle$ in equation (2), rather than the SO coupling, one obtains an effective Dirac equation for a particle with a spatially random mass. This model, also known as the FGM [25, 26], is characterized by a Dyson singularity in the DOS [38], which is a consequence of the chiral symmetry of equation (2) without kinetic energy, and which leads to a power-law dependence of the correlation function. The absence of any exponential contribution to the correlation functions can most easily be seen by considering the divergent behavior of the localization length $L_{\mathrm{loc}}(E) = 1/\gamma(E)$ as a function of the energy E, which is inversely proportional to the Lyapunov exponent $\gamma(E)$. The latter one is related to the integrated DOS $N(E)$ by the Kramers–Kronig relation [39]

$$\gamma(E) = \frac{1}{\pi} \int \mathrm{d}E' \frac{N(E')}{E' - E}, \tag{4}$$

where

$$N(E) \sim \frac{1}{\ln^2 |E|}. \tag{5}$$

The DOS $\rho(E) = \mathrm{d}N/\mathrm{d}E$ of the FGM exhibits a singular behavior when approaching the band-center, i.e. $E \to 0$, known as the Dyson singularity introduced above [22]. Putting everything together implies that the localization length $\zeta(E \approx 0)$ exhibits a logarithmic divergence as the energy E approaches the band center.

Let us now discuss a possible experimental realization based on ^{87}Rb atoms. First, we discuss how to single out the tripod linkage pattern (cf figure 3(a). We choose the ground-states as $|1\rangle = |F = 2, m_{\mathrm{F}} = -1\rangle$, $|2\rangle = |F = 2, m_{\mathrm{F}} = +1\rangle$ and $|3\rangle = |F = 1, m_{\mathrm{F}} = 0\rangle$ of the $5S_{1/2}$ ground-state manifold of Rb. These states are coupled via $\sigma^{\pm}$ polarized ($\Omega_{1,2}$) or π-polarized light (Ω_3), respectively, to the excited state $|0\rangle = |F = 2, m_{\mathrm{F}} = 0\rangle$ of the $5P_{1/2}$-manifold. To prevent the coupling fields from driving other transitions we apply an additional magnetic field to induce a Zeeman splitting of the different m_{F}-states which due to different Landé-g_{F}-factors will be shifted out of resonance. It should be noted that a generalization to a multiple-state configuration including all Zeeman-levels or a different choice of states are possible and have been experimentally realized [42, 43].

Let us now address the generation of the disorder potential. These can be created using speckle potentials [13, 36] or incommensurate optical lattices [14], which induce spatially varying ac-Stark shifts. Denoting the amplitude of the speckle potential Ω_{ac}, it is easy to see that for far off-resonant dressing of the atoms with Ω_{ac} the ground-states experience an ac-Stark-shift proportional to $\Omega_{\mathrm{ac}}^2/\Delta$ (for states $|1\rangle$, $|2\rangle$) and $\Omega_{\mathrm{ac}}^2/\Delta'$ (for state $|3\rangle$), where Δ and Δ' denote the detunings of the speckle field from the respective resonance. Note that the signs of the two shifts are opposite for states $|1\rangle$, $|2\rangle$ and $|3\rangle$ if $\mathrm{sgn}(\Delta) = -\mathrm{sgn}(\Delta')$ (cf figure 3(b)). This can easily be achieved in ^{87}Rb as the hyper-fine energy splitting in the $5S_{1/2}$-manifold is substantially larger than in the $5P_{1/2}$-manifold. This results in an opposite sign of the potential

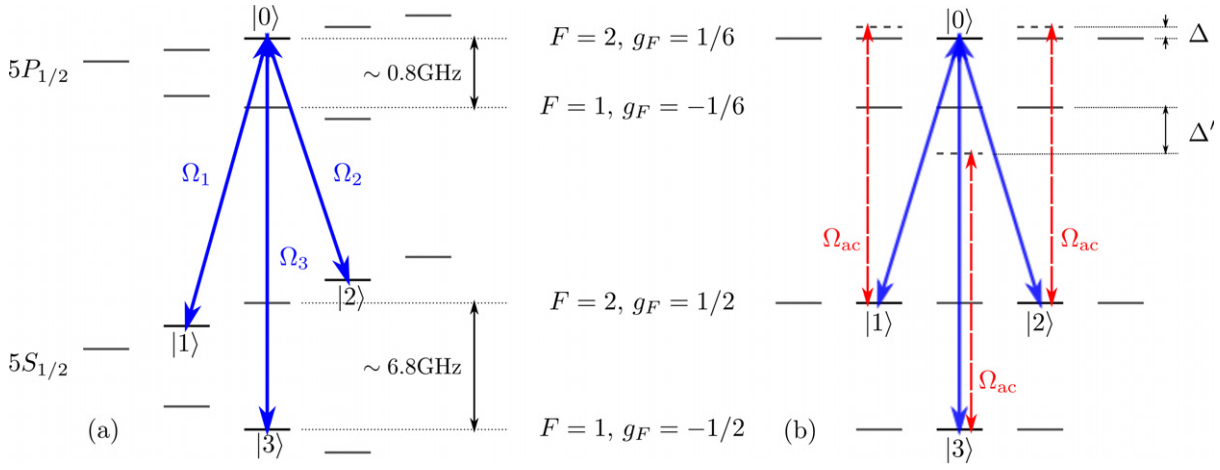

Figure 3. (a) Experimental implementation in ^{87}Rb. A homogeneous magnetic field creates different Zeeman splittings in the hyperfine manifolds to isolate a single tripod-linkage pattern. (b) Off-diagonal disorder with $V_- = V_2$ is created by a single field Ω_{AC}. Opposite, large detunings Δ and Δ' lead to opposite signs of the ac-Stark shifts of states $|1\rangle$ and $|2\rangle$ with respect to that of state $|3\rangle$. Disorder is created by a spatially fluctuating amplitude of Ω_{AC} realized, e.g. by a speckle pattern.

for the dark-states necessary to generate the mass-disorder for the spinors. Any finite offset of the mass can be eliminated by an additional two-photon detuning of the coupling fields $\Omega_{1,2,3}$. Note that the fields generating the disorder do not contribute to the generation of the dark-states and hence do not induce any non-adiabatic dynamics in the dark-state subspace. Finally, the angle θ, which governs the effective strength of the SO coupling, depends only on the ratio of the Rabi frequencies and as such it is insensitive to overall amplitude fluctuations as long as the fields are derived from the same source.

3. Density of states for tripod-coupled atoms with disorder

We now consider the role of the DOS of the SO-coupled system with off-diagonal disorder, equation (2), to investigate what determines the crossover from Anderson-like to anomalous localization. In the case of a random potential it is not immediately obvious in which parameter regimes equation (2) leads to Schrödinger- or Dirac-like dynamics. To answer this question we introduce dimensionless units $\xi = \Gamma x/v_D$ and $\tau = \Gamma t$, resulting in

$$\mathrm{i}\frac{\partial}{\partial\tau}\mathbf{\Psi} = -\frac{\Gamma}{2mv_D^2}\frac{\partial^2}{\partial\xi^2}\mathbf{\Psi} - \mathrm{i}\cos\theta\hat{\sigma}_x\frac{\partial}{\partial\xi}\mathbf{\Psi} + \tilde{\Delta}(\xi)\hat{\sigma}_z\mathbf{\Psi}, \tag{6}$$

where $\tilde{\Delta}(\xi) = \Delta/\Gamma$. In the following we analyze the DOS in the system described by equation (6). For a free Schrödinger particle the DOS has a singularity at $\omega = 0$. As can be seen from figure 2, the presence of the SO coupling shifts the band-edge of the spectrum away from zero to $\omega_{edge} = -mc_*^2/2 = -mv_D^2\cos^2\theta/2$. In the Dirac limit $mv_D^2 \to \infty$ the band edge moves to infinity. In the pure Schrödinger case weak disorder leads to a smoothing of the band-edge peak [40], making the DOS analytic, which is associated with the emergence of exponentially

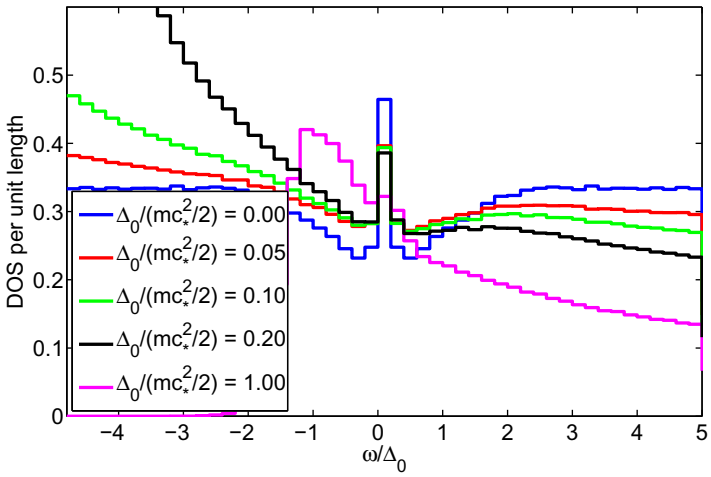

Figure 4. DOS per unit length for a SO-coupled massive Schrödinger particle in a random potential with a finite disorder correlation length (see footnote 6) for various values of the band edge mc_*^2. As the band edge is moving closer to $\omega = 0$ the washing out of the Dyson singularity of the free Dirac case (blue line) becomes more prominent, until the almost purely disordered Schrödinger case (magenta line) is reached.

localized states (Anderson localization) [41]. To investigate the DOS for our SO-coupled system in the presence of disorder we numerically simulate equation (6). As will be the case in any experiment we assume for this a discretized model and furthermore a finite disorder-correlation length[6]. (A smaller correlation length is accompanied by slower numerical convergence of the DOS [25].) The mobility edge in momentum space associated with the finite disorder correlation length is however chosen large enough not to affect the results. Figure 4 shows the DOS for different values of the dimensionless quantity Δ_0/mc_*^2, where Δ_0 characterizes the rms value of the Gaussian disorder amplitude in the discretized model. It is related to the continuum quantity via $\Gamma = \Delta_0^2/(v_D n_{\text{kinks}})$, with n_{kinks} being the impurity density.

For $mc_*^2 \to \infty$, i.e. in the Dirac limit, one recognizes a Dyson-like singularity at $\omega = 0$. The emergence of a Dyson singularity can in general be taken as an indicator for anomalous, i.e. non-exponential, localization properties [22]. In the random-mass Dirac model or FGM the Dyson singularity has been shown to lead to power-law correlations [23]. As $mc_*^2 \sim m v_D^2 \cos^2\theta$ decreases the band-edge approaches the singularity and as a consequence the singularity is smoothed out. It should be noted at this point that a true singularity is present only in the exact Dirac limit, but as can be seen from figure 4 a pronounced peak survives as long as the SO coupling, i.e. mc_*^2, is sufficiently large. Thus one expects in this case a localization scenario where power-law correlations dominate for very long time scales. To quantify this we define, following [25], the width $\Delta\omega_D$ of the Dyson singularity as the minimum of the DOS, yielding $\Delta\omega_D = \alpha\Gamma$, where $\alpha = 0.6257\ldots$. Hence, to obtain dynamics associated with the Dyson singularity the condition

$$m v_D^2 \cos^2\theta \gg \Gamma \tag{7}$$

[6] For the numerics we used an exponentially correlated disorder according to $\overline{\Delta_i \Delta_j} = \Delta_0^2 \Delta x / L_{\text{corr}} \exp\{-|i-j|\Delta x/2L_{\text{corr}}\}$ with correlation length $L_{\text{corr}} = 2\Delta x$, where Δx is the discretization length.

should be satisfied in order to ensure that the band-edge is sufficiently far away from the singularity.

The emergence of the Dyson singularity affects the dynamics of the system around $\omega = 0$. Experimentally this is reflected in a drastically different behavior of the density profile after a long-time expansion of an initially localized wave-packet. From equation (7) we expect that for $\cos^2\theta \gg \Gamma/mv_D^2$ the effective Dirac dynamics along with the creation of anomalous power-law correlations dominates the system, whereas in the opposite limit we expect Anderson-like localization. The power-law behavior of correlations will also be reflected in the density distribution of an expanding wavepacket, which is an important experimentally measurable quantity. To see this, we note that in the power-law case there is no intrinsic length scale. Thus we may assume that an initially well localized wave-packet will show the same behavior as a wavepacket with an initial delta-distribution $\Psi(x, t = 0) = \delta(x)\boldsymbol{\chi}$, with $\boldsymbol{\chi}$ being a constant vector of unity length. The time-evolution of this wave-packet is given by $\Psi(x, t) = \sum_n [\boldsymbol{\phi}_n^*(0) \cdot \boldsymbol{\chi}]\boldsymbol{\phi}_n(x)\, e^{-i\omega_n t}$, where $\boldsymbol{\phi}_n(x)$ is the stationary state of a particular disorder realization belonging to the state of energy ω_n. It immediately follows that the long-time evolution is given by $\overline{|\Psi(x, t \to \infty)|^2} = \sum_n \overline{|\boldsymbol{\phi}_n(0)|^2 |\boldsymbol{\phi}_n(x)|^2}$. The right hand side of this expression corresponds to the localization criterion defined in [22], and it is thus sufficient to investigate the long-time behavior of the density in order to determine localization properties. In the Schrödinger limit all correlations of the type $C_n(x) = \overline{|\boldsymbol{\phi}_n(0)|^2 |\boldsymbol{\phi}_n(x)|^2}$ decay exponentially [22], i.e. $C_n(x) \sim e^{-|x|/L_{\mathrm{loc}}}$, where the localization length L_{loc} is at most of the order of the system size. In the FGM the typical localization length of correlation functions scales as $L_{\mathrm{loc}} \sim |\ln \epsilon|^2$ [24], where ϵ is the distance from the band-center. For small energies this length is much larger than the system size and consequently the correlation functions should be similar to the zero-energy correlation function decaying with a power law scaling as $C_n(x) \sim (\Gamma|x|/v_D)^{-3/2}$ at large distances [24]. Accordingly, one expects quite different scaling behavior in the two different limits of large and small SO coupling.

4. Wavepacket dynamics

To confirm the predictions of the previous section we numerically simulated the time-evolution according to equation (2) of an initially localized wave-packet of the form $\Psi(x, t = 0) = (2\sqrt{2\pi}L_0 \operatorname{erf}(L/\sqrt{2}L_0))^{-1/2} \exp(-x^2/4L_0^2)(1, i)^{\mathrm{T}}$ of width L_0 in a system of total length $2L$. The results, shown in figure 5, depict the density profile for different SO coupling strengths and $\Gamma/mv_D^2 = 0.1$ after a sufficiently long time evolution T. For $\cos\theta = (0.01, 0.05)$ one can clearly see the exponentially localized wings of the density reminiscent of Anderson localization in cold atom systems [13, 14, 37]. Increasing the SO coupling strength leads to an intermediate regime at $\cos\theta = 0.5$ where neither exponential nor power-law localization can be determined. Finally, for strong SO coupling, i.e. $\cos\theta = 1$ a fit with a power-law reveals that the density correlation scales as the expected $3/2$ power-law at large distances in agreement with the predictions of the FGM.

To understand the $3/2$ power-law exponent and show its connection to the formation of a zero-energy state, we perform a gauge transformation of equation (2) with $\Psi = \exp(-imc_* x\hat{\sigma}_x)\boldsymbol{\Phi}$, giving:

$$i\frac{\partial \Phi}{\partial t} = -\frac{1}{2m}\frac{\partial^2}{\partial x^2}\Phi - \frac{1}{2}mc_*^2\Phi + \Delta(x)[\hat{\sigma}_z \cos(2mc_* x) + \hat{\sigma}_y \sin(2mc_* x)]\Phi, \qquad (8)$$

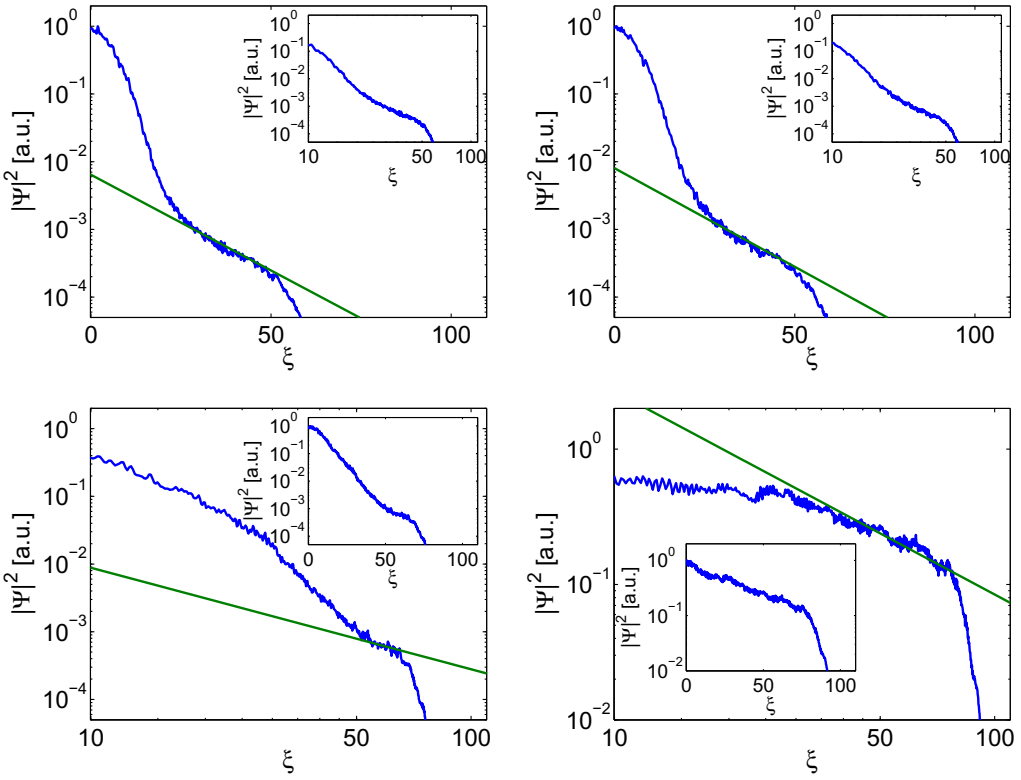

Figure 5. Density profiles of an initially localized wave packet of size $L_0\Gamma/v_D = 7.5$ after a time evolution $\Gamma t = 80$ according to equation (6) with $\Gamma/mv_D^2 = 0.1$ after averaging over 100 independent realizations. The system size is $2L\Gamma/v_D = 240$ and $n_{\text{kinks}} = 6.25\Gamma/v_D$, i.e. $\Delta_0^2/\Gamma^2 = 6.25$. Top left, right: Schrödinger limit with $\cos\theta = (0.01, 0.05)$. The green (straight) line corresponds to an exponential fit showing the expected Anderson localization. The inset shows the same density in log-log. Bottom left: density in the crossover regime with $\cos\theta = 0.5$ in log-log representation (semi-log in the inset) and a power-law fit (green straight line) with exponent 3/2. Bottom right: Dirac limit with $\cos\theta = 1$ in log–log; the power-law behavior is clearly visible for large distances $\xi \gg 1$.

and subsequently substitute the Ansatz $\mathbf{\Phi} = \boldsymbol{\chi}_+ \exp(imc_*x) + \boldsymbol{\chi}_- \exp(-imc_*x)$ into equation (8), yielding

$$\mathrm{i}\left(\frac{\partial\chi_+}{\partial t}\mathrm{e}^{\mathrm{i}\eta} + \frac{\partial\chi_-}{\partial t}\mathrm{e}^{-\mathrm{i}\eta}\right) = \Delta(x)(\hat{\sigma}_z\cos(2\eta)\chi_+\mathrm{e}^{\mathrm{i}\eta} + \hat{\sigma}_z\cos(2\eta)\chi_-\,\mathrm{e}^{-\mathrm{i}\eta} + \hat{\sigma}_y\sin(2\eta)\chi_+\mathrm{e}^{\mathrm{i}\eta} + \hat{\sigma}_y\sin(2\eta)\chi_-\,\mathrm{e}^{-\mathrm{i}\eta}) - \frac{1}{2m}\left(\frac{\partial^2\chi_+}{\partial x^2}\mathrm{e}^{\mathrm{i}\eta} + \frac{\partial^2\chi_-}{\partial x^2}\mathrm{e}^{-\mathrm{i}\eta}\right) + ic_*\left(\frac{\partial}{\partial x}\chi_-\,\mathrm{e}^{-\mathrm{i}\eta} - \frac{\partial}{\partial x}\chi_+\mathrm{e}^{\mathrm{i}\eta}\right), \tag{9}$$

with $\eta = mc_*x$. We can simplify equation (9) by dropping terms proportional to $\partial_x^2\chi_\pm$ and fast oscillating exponentials using the assumption $\Gamma/mv_D^2 \ll \cos^2\theta$. This gives the equation

$$\mathrm{i}\frac{\partial\boldsymbol{\chi}}{\partial t} = -\mathrm{i}c_*\hat{\tau}_z\otimes\mathbb{1}\frac{\partial\boldsymbol{\chi}}{\partial x} + \frac{\Delta(x)}{2}\left(\hat{\tau}_x\otimes\hat{\sigma}_z + \hat{\tau}_y\otimes\hat{\sigma}_y\right)\boldsymbol{\chi}. \tag{10}$$

Here we defined the four-component object $\boldsymbol{\chi} = (\boldsymbol{\chi}_+, \boldsymbol{\chi}_-)^T$ and $\hat{\sigma}_i$, $\hat{\tau}_i$, $i \in \{x, y, z\}$, act on the momentum or internal degree of freedom, respectively. Equation (10) is a generalization of the model considered in [23, 24]. It possesses a zero-energy (mid-gap) state given by $\boldsymbol{\chi}(x) \sim \exp\{\pm\hat{\alpha}/2c_* \int_{-\infty}^{x} \mathrm{d}y\Delta(y)\}\boldsymbol{\chi}_0$. The matrix $\hat{\alpha} = (\hat{\tau}_y \otimes \hat{\sigma}_z + \hat{\tau}_x \otimes \hat{\sigma}_y)$ has eigenvalues $(1, -1, 0, 0)$. Choosing $\boldsymbol{\chi}_0$ to be an eigenvector with eigenvalue ± 1 we obtain a power-law intensity correlation scaling as $C(x) \sim (\Gamma|x|/v_\mathrm{D})^{-3/2}$ [23, 24] in full agreement with the numerical simulations.

5. Conclusions

In summary, we have investigated the 1D dynamics of a SO-coupled massive Schrödinger particle subject to a δ-correlated disorder potential. For weak SO coupling the system is equivalent to two independent Schrödinger particles with diagonal disorder. In the opposite limit the system is described by the random-mass Dirac model with off-diagonal disorder. The model can be implemented with current state-of-the-art techniques by using atomic dark-states in cold atom systems. We showed by calculating the systems' DOS and direct numerical simulation of the time evolution of an expanding wave packet that there is a crossover from an exponential (Anderson) localized regime to a power-law regime governed by a Dyson singularity when varying the strength of the SO coupling relative to the disorder strength. The crossover can be observed by expansion of an initially localized wavepacket with an appropriately chosen width of the momentum distribution in a random potential. Future investigations should include interaction effects, which will allow the study of models such as the relativistic Thirring model [44] for fermions as well as for bosons with a random mass. Interactions may well accelerate the crossover to non-exponential behavior as they tend to delocalize particles. It is also interesting to investigate whether the model can be recast in terms of a critical theory to study the nature of the crossover.

Acknowledgments

We thank B Halperin, C Hooley, M Merkl and D Muth for useful discussions. We acknowledge support from the EPSRC Scottish Doctoral Training Centre in Condensed Matter Physics (MJE), the DFG through the project UN 280/1 (RGU), the SFB TR49 (MF) and the Harvard Quantum Optics Center (JO).

References

[1] Bloch I, Dalibard J and Zwerger W 2008 *Rev. Mod. Phys.* **80** 885
[2] Jaksch D *et al* 1998 *Phys. Rev. Lett.* **81** 3108
[3] Morsch O and Oberthaler M 2006 *Rev. Mod. Phys.* **78** 179
[4] Fetter A L 2009 *Rev. Mod. Phys.* **81** 647
[5] Giorgini S, Pitaevskii L P and Stringari S 2008 *Rev. Mod. Phys.* **80** 1215
[6] Juzeliūnas G and Öhberg P 2004 *Phys. Rev. Lett.* **93** 033602
[7] Dalibard J *et al* 2011 *Rev. Mod. Phys.* **83** 1523
[8] Lin Y-J, Jimenez-Garcia K and Spielman I B 2011 *Nature* **471** 83
[9] Campbell D L, Juzeliūnas G and Spielman I B 2011 arXiv:1102.3945
[10] Juzeliūnas G *et al* 2008 *Phys. Rev.* A **77** 011802

[11] Merkl M *et al* 2008 *Europhys. Lett.* **83** 54002
[12] Anderson P W 1958 *Phys. Rev.* **109** 1492
[13] Billy J *et al* 2008 *Nature* **453** 891
[14] Roati G *et al* 2008 *Nature* **453** 895
[15] Cutler M and Mott N F 1969 *Phys. Rev.* **181** 1336
[16] Wiersma D S *et al* 1997 *Nature* **390** 671
[17] Dalichaouch R *et al* 1991 *Nature* **354** 53
[18] Weaver R L 1990 *Wave Motion* **12** 129
[19] Gogolin A A 1982 *Phys. Rep.* **86** 1
[20] Fabrizio M and Melin R 1997 *Phys. Rev. Lett.* **78** 3382
[21] Unanyan R G *et al* 2010 *Phys. Rev. Lett.* **105** 173603
[22] Lifshits I M, Gredeskul S A and Pastur L A 1988 *Introduction to the Theory of Disordered Systems* (New York: Wiley)
[23] Shelton D G and Tsvelik A M 1998 *Phys. Rev.* B **57** 14242
[24] Balents L and Fisher M P A 1997 *Phys. Rev.* B **56** 12970
[25] Millis A J and Monien H 2000 *Phys. Rev.* B **61** 12496
[26] Bartosch L and Kopietz P 1999 *Phys. Rev.* B **60** 15488
[27] Dyson F J 1953 *Phys. Rev.* **92** 1331
[28] Smith E R 1970 *J. Phys. C: Solid State Phys.* **3** 1419
[29] Theodorou G and Cohen M H 1976 *Phys. Rev.* B **13** 4597
[30] Eggarter T P and Riedinger R 1978 *Phys. Rev.* B **18** 569
[31] Fleishman L and Licciardello D C 1977 *J. Phys. C: Solid State Phys.* **10** L125
[32] Zhu S L, Zhang D W and Wang Z D 2009 *Phys. Rev. Lett.* **102** 210403
[33] Unanyan R G *et al* 1998 *Opt. Commun.* **155** 144
[34] Berry M V 1984 *Proc. R. Soc.* A **394** 45
[35] Mead C A 1992 *Rev. Mod. Phys.* **64** 51
[36] Clement D *et al* 2006 *New J. Phys.* **8** 165
[37] Sanchez-Palencia L *et al* 2007 *Phys. Rev. Lett.* **98** 210401
[38] Ovchinnikov A A and Erikhman N S 1977 *Zh. Eksp. Teor. Fiz.* **73** 650
[39] Pastur L and Figotin A 1991 *Spectra of Random and Almost-Periodic Operators* (New York: Springer)
[40] Halperin B I 1965 *Phys. Rev.* **139** A104
[41] Bouchaud J P, Comtet A and Georges A 1990 *Ann. Phys.* **201** 285
[42] Karpa L, Vewinger F and Weitz M 2008 *Phys. Rev. Lett.* **101** 170406
[43] Wang H *et al* 2011 *Phys. Rev.* A **83** 043815
[44] Thirring W E 1958 *Ann. Phys.* **3** 91